CONVERSION OF CESR TO HIGH BRIGHTNESS X–RAY SOURCE

R. Talman, JLAB, 29 September, 2005

1.

TOPICS FOR THIS TALK

Why Bright X–Rays?

- Phase contrast imaging, x–ray holography, microbeams, etc. etc.

Implication For Electron Beam?

- Low emittance, $\epsilon^{(N)} <\sim 1\,\mu$m, fairly high energy. e.g. 5 GeV

Possible Routes:

ENERGY RECOVERY LINAC (ERL)

I string space charge formulation

- Start with small emittance and preserve it through acceleration
- why recover energy?
- advantages
  - potential for very small emittance from linac
  - potential for ultrashort (femtosec) pulses
- disadvantages
  - expensive, high power
  - emittance growth due to CSR (coherent synchrotron radiation) and CSCF (centrifugal space charge force)

II CESR upgrade

(FAST CYCLING) CONVENTIONAL LIGHT SOURCE

- Start with arbitrary emittance and cool by synchrotron radiation
- advantages
  - continuity of time, scale, and personel
  - conventional technology
  - little new conventional construction
  - symbiosis with linear collider damping ring design
- disadvantages
  - ultrashort bunch operation is impossible
  - at most two long undulators can be accomodated

PRST-AB 7, 100701 (2004)

STRING/POINT CHARGE REFORMULATION OF SPACE CHARGE FORCE

- Fundamental problem: Coulomb 1/r^2 and near collisions

- represent space charge force as force between point and longitudinal 'string'
- longitudinal force corresponds to coherent synchrotron radiation (CSR)
  - after regularization to remove (only logarithmic) divergence, self–work on bunch matches integrated Poynting power!
  - causes particle energy to depend on position along bunch, indirectly giving emittance growth
- transverse force is "centrifugal space charge force" (CSCF)
  - gives direct emittance growth

- formulation of space charge problem as 'intrabeam scattering'

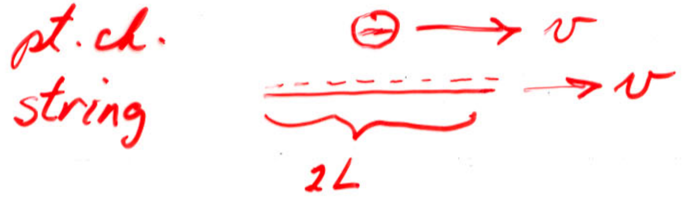


# String Formulation of Space Charge Forces in a Deflecting Bunch

PRST-AB 7, 100701 (2004)

Richard Talman
*Laboratory of Elementary-Particle Physics, Cornell University, Ithaca, NY, USA*

(Dated: January, 2004)

erratic close encounters

The force between two moving point charges, because of its inverse square law singularity, cannot be applied directly in the numerical simulation of bunch dynamics; radiative effects make this especially true for short bunches being deflected by magnets. This paper describes a formalism circumventing this restriction in which the basic ingredient is the *total* force on a point charge co-moving with a longitudinally-aligned, uniformly-charged string. Bunch evolution can then be treated using direct particle-to-particle, intrabeam scattering, with no need for an intermediate, particle-in-cell, step. Electric and magnetic fields do not appear individually in the theory. Since the basic formulas are both exact (in paraxial approximation) and fully relativistic, they are applicable to beams of all particle types and all energies. But the theory is expected to be especially useful for calculating the emittance growth of the ultrashort electron bunches of current interest for ERL's (energy recovery linacs) and FEL's (free electron lasers). The theory subsumes CSR (coherent synchrotron radiation) and CSCF (centrifugal space charge force.) Renormalized, on-axis, longitudinal field components are in excellent agreement with values from Saldin et al.[1]

no PIC

In a numerical simulation of bunch dynamics, each of the $N$ particles is to be treated as a point particle as far as its own dynamics is concerned, but as a line charge for the purpose of calculating the electromagnetic fields it generates. The forces caused by these fields can either be applied directly to each individual particle in the bunch or, for simulations in which $N$ is very large, be recorded on a three dimensional grid, from which forces on individual particles are then calculated by interpolation. In either case the basic ingredient is the force on a point charge due to a charged string.

intrabeam scattering

effective field

no P.I.C.

# Self-Force of Moving Line Charge ("string")

- can use retarded $\Phi, \mathbb{A}$, but getting $\mathbb{E}$ + $\mathbb{B}$ is hard
- can use $\underbrace{\text{retarded } \mathbb{E}, \mathbb{B}}_{\text{simple electro-magneto-statics}}$, but must include end terms

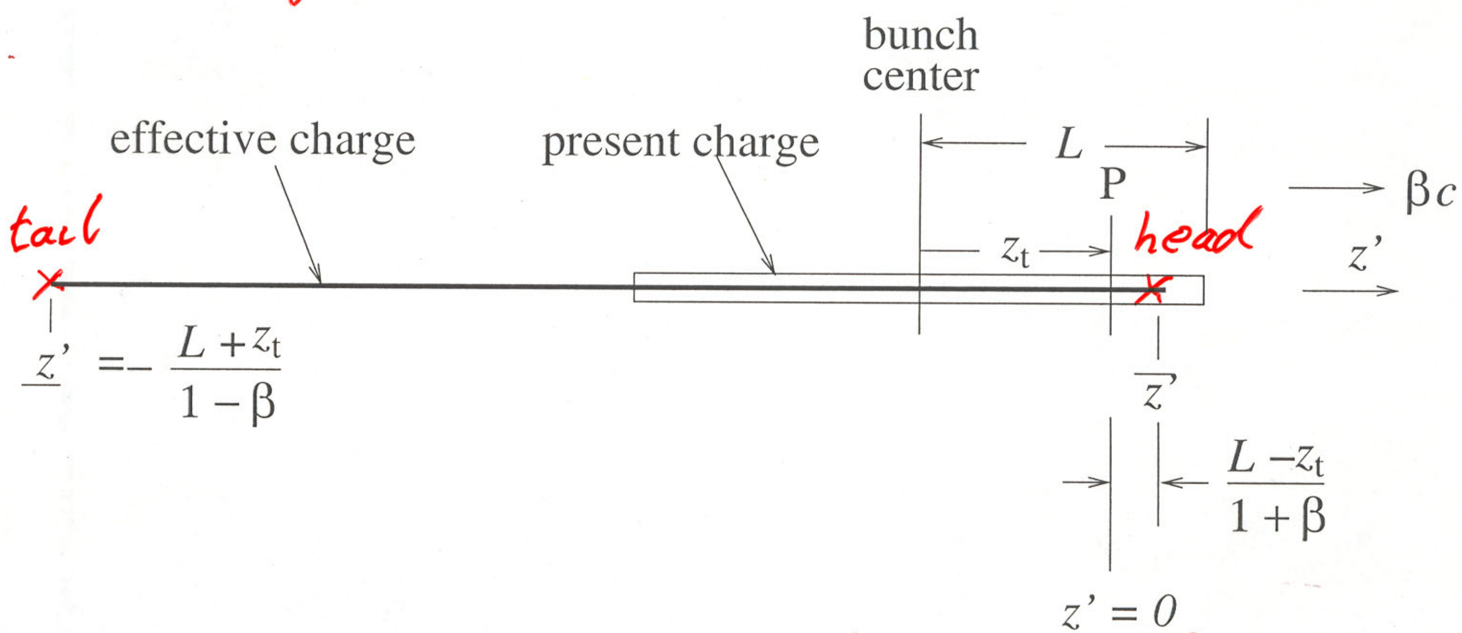


- string tension is infinite (unphysical)
- but only logarithmic
- total self-force vanishes

# Off-axis fields

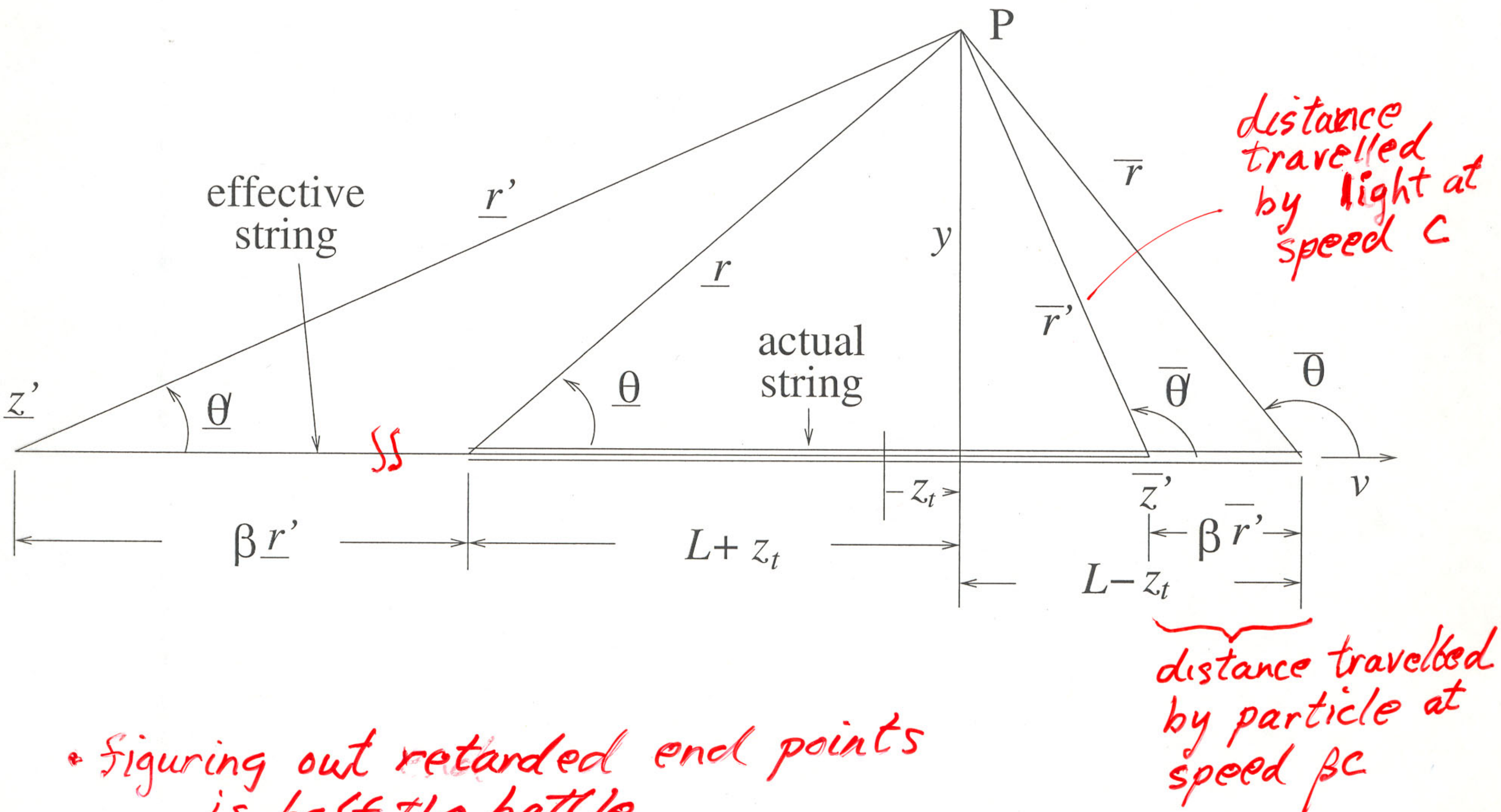


• figuring out retarded end points is half the battle

# Curving Line Charge

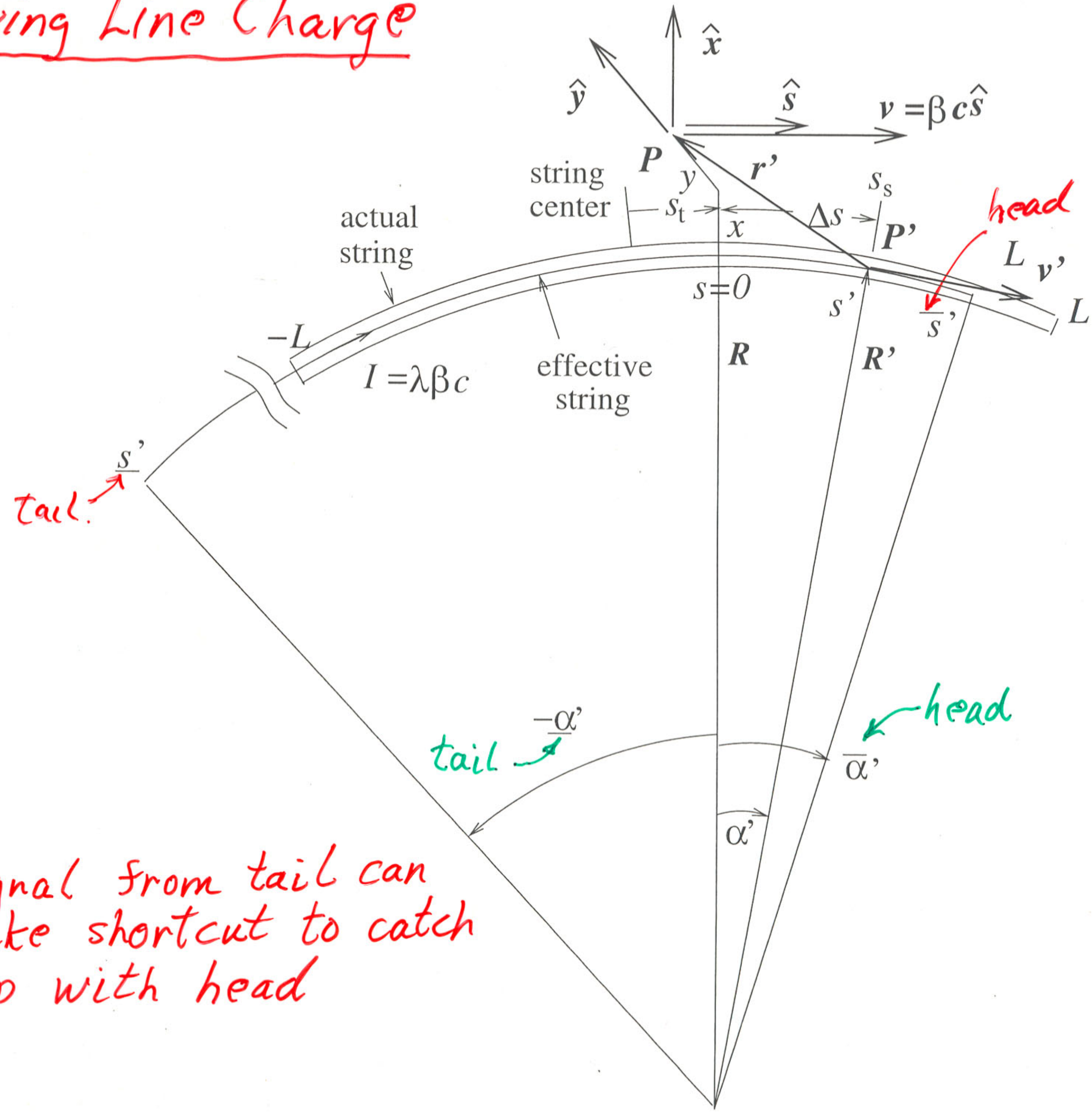


- signal from tail can take shortcut to catch up with head

7

Force Law (closed form).

$$\kappa = 1 - \beta\hat{\mathbf{v}}' \cdot \hat{\mathbf{r}}' = 1 + \beta \sin\alpha' \frac{R+x}{r'}.$$

Spelling out the components, the $\gamma$-independent part is

"ends"

$$\frac{\mathbf{F}_0^{(\mathrm{ends})}}{e} = \frac{\beta\lambda_0}{4\pi\epsilon_0}\left[\frac{1-\cos\alpha'}{\kappa r'^2}\begin{pmatrix} -R\sin\alpha' \\ R(1-\cos\alpha')+x \\ y\end{pmatrix} - \frac{R\sin\alpha' + \beta r'}{\kappa r'^2}\begin{pmatrix}\cos\alpha' \\ -\sin\alpha' \\ 0\end{pmatrix}\right]$$

$z$ $x$ $y$

$$= \frac{\beta\lambda_0}{4\pi\epsilon_0}\left[\begin{matrix} -R\sin\alpha'/\kappa r'^2 - \beta\cos\alpha'/\kappa r' \\ (2R+x)(1-\cos\alpha')/\kappa r'^2 + \beta\sin\alpha'/\kappa r' \\ (1-\cos\alpha')\,y/\kappa r'^2\end{matrix}\right]_{\underline{\alpha}'}^{\overline{\alpha}'}.$$

The $1/\gamma^2$ term in Eq. (77) will typically be negligible but, if needed, it is

$$\frac{\mathbf{F}_{1/\gamma^2}^{(\mathrm{ends})}}{e} = \frac{\beta\lambda_0}{4\pi\epsilon_0\gamma^2}\begin{pmatrix} 0 \\ R(\cos\alpha'-1)+x\cos\alpha' \\ y\cos\alpha'\end{pmatrix}$$

"body"

$$\frac{\mathbf{F}_0^{(\mathrm{body})}}{e} = \frac{R\lambda_0}{4\pi\epsilon_0}\int_{\underline{\alpha}'}^{\overline{\alpha}'}\frac{d\alpha'}{r'^3}\left[(1-\cos\alpha')\begin{pmatrix} -R\sin\alpha' \\ R(1-\cos\alpha')+x \\ y\end{pmatrix} - R\sin\alpha'\begin{pmatrix}\cos\alpha' \\ -\sin\alpha' \\ 0\end{pmatrix}\right]$$

$$= \frac{R\lambda_0}{4\pi\epsilon_0}\int_{\underline{\alpha}'}^{\overline{\alpha}'} d\alpha'\begin{pmatrix} -R\sin\alpha'/r'^3 \\ (2R+x)(1-\cos\alpha')/r'^3 \\ (1-\cos\alpha')\,y/r'^3\end{pmatrix}$$

and the components of $\mathbf{F}_{1/\gamma^2}^{(\mathrm{body})}$ are

$$\frac{\mathbf{F}_{1/\gamma^2}^{(\mathrm{body})}}{e} = \frac{R\lambda_0}{4\pi\epsilon_0\gamma^2}\int_{\underline{\alpha}'}^{\overline{\alpha}'}\frac{d\alpha'}{r'^3}\left[\cos\alpha'\begin{pmatrix} -R\sin\alpha' \\ R(1-\cos\alpha')+x \\ y\end{pmatrix} + R\sin\alpha'\begin{pmatrix}\cos\alpha' \\ -\sin\alpha' \\ 0\end{pmatrix}\right]$$

$$= \frac{R\lambda_0}{4\pi\epsilon_0\gamma^2}\int_{\underline{\alpha}'}^{\overline{\alpha}'} d\alpha'\begin{pmatrix} 0 \\ (-R(1-\cos\alpha')+x\cos\alpha')/r'^3 \\ y\cos\alpha'\,/r'^3\end{pmatrix}$$

8

CLOSED FORM

## X. EVALUATION OF INTEGRALS

The end effect forces have been given in closed form and the longitudinal body force integral evaluated for $x = 0$. For $x \neq 0$ the integals can also be evaluated in closed form, but they are more complicated. Depending, as they do, on $r'$ as given by Eq. (53), the integrals appearing in Eqs. (72) and (73) depend on factors

$$\begin{aligned} \mathrm{E}(z,k) &= \int_0^z \sqrt{1-k^2t^2}/\sqrt{1-t^2}\,dt, \\ \mathrm{F}(z,k) &= \int_0^z 1/\sqrt{(1-k^2t^2)(1-t^2)}\,dt, \\ \mathrm{Pi}(z,\nu,k) &= \int_0^z 1/\sqrt{(1-\nu t^2)(1-t^2)(1-k^2t^2)}\,dt \end{aligned} \tag{99}$$

elliptic integrals. (quick algorithms are available)

$$\begin{aligned} I_s &= \int \frac{\sin\alpha'}{(A+B\,\cos\alpha')^{3/2}}\,d\phi = \frac{2}{B\sqrt{A+B\cos\alpha'}}, \qquad I_0 = \int \frac{\cos\alpha'}{(A+B\,\cos\alpha')^{3/2}}\,d\phi, \\ I_{x,y} &= \int \frac{1-\cos\alpha'}{(A+B\,\cos\alpha')^{3/2}}\,d\phi \\ &= 2\,\frac{-B\sin(\alpha')+\sqrt{A-B}\,\sqrt{A-B+2B\cos^2(\alpha'/2)}\left(\mathrm{F}\big(\cos(\alpha'/2),\sqrt{\tfrac{-2B}{A-B}}\big)-\mathrm{E}\big(\cos(\alpha'/2),\sqrt{\tfrac{-2B}{A-B}}\big)\right)}{\sqrt{A-B+2B\cos^2(\alpha'/2)}\,B(A-B)} \end{aligned} \tag{100}$$

It is even possible to integrate first over $y$;

$$\begin{aligned} II_s &= \int d\phi \int dy \frac{\sin\alpha'}{(A+B\,\cos\alpha')^{3/2}} = \frac{1}{2R(R+x)}\ln\frac{\sqrt{2R(R+x)+x^2+y^2-2R(R+x)\cos\alpha'}-y}{\sqrt{2R(R+x)+x^2+y^2-2R(R+x)\cos\alpha'}+y} \\ II_x &= \int d\phi \int dy \frac{1-\cos\alpha'}{(A+B\,\cos\alpha')^{3/2}} \\ &= -y\frac{x^2\Big(\mathrm{F}\big(\cos(\alpha'/2),D\big)-\mathrm{Pi}\big(\cos(\alpha'/2),C,D\big)\Big)+4R(R+x)\mathrm{F}\big(\cos(\alpha'/2),D\big)}{R(R+x)(x+2R)^2\sqrt{4R(R+x)+x^2+y^2}} \end{aligned} \tag{101}$$

would be appropriate for "ribbons"

where

$$C = \frac{4R(R+x)}{(x+2R)^2}, \quad D = 2\sqrt{\frac{R(R+x)}{4R(R+x)+x^2+y^2}}. \tag{102}$$

~~20~~ ~~21~~ ~~22~~ 9

# Pictorial Representation of Renormalization

- for comparing self-work with Poynting energy radiated

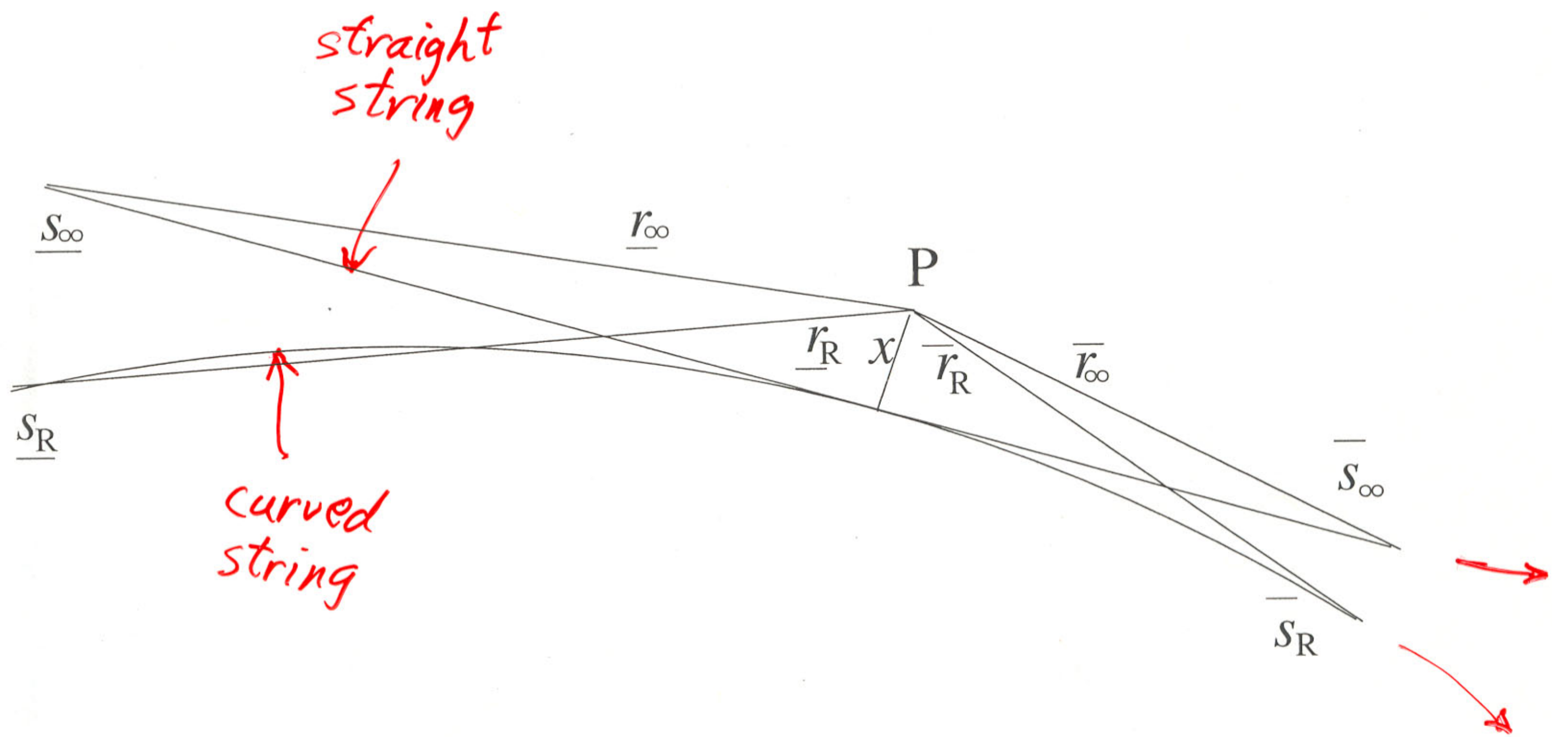


- not needed for simulation code
- i.e. regular space charge force, CSR, and CSCF are all subsumed into point charge/string charge force

# Comparison With Saldin et. al. (almost indistinguishable)

- on-axis only

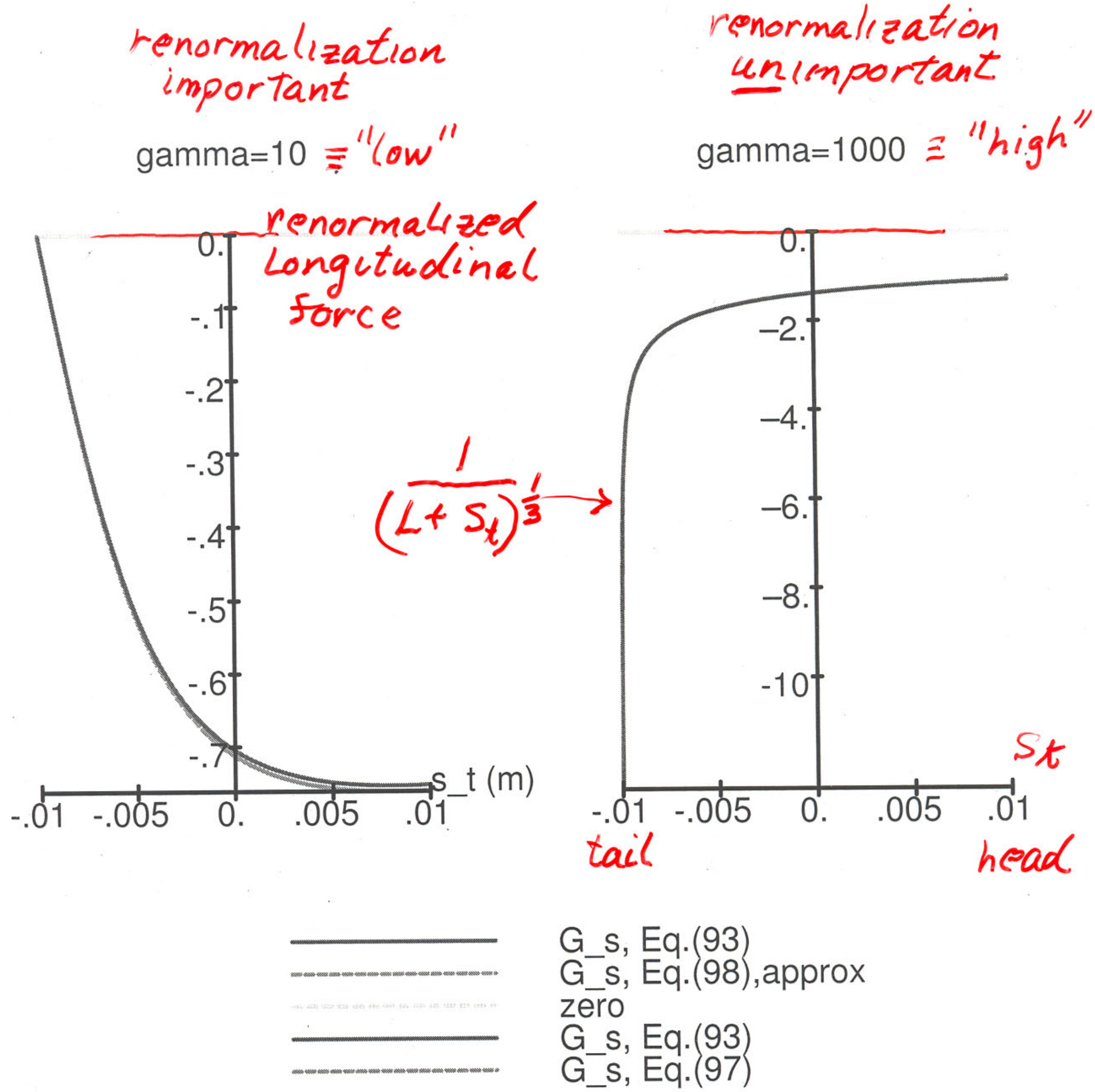


- theory presented is valid everywhere
- " " includes transverse force

Check against CSR

TABLE I: Coherent power, as calculated by self-force, $P$, and as by Schwinger from far fields, $P^{(N)}_{\text{coh.}}$. $L = 0.01\,\text{m}$, $R = 10\,\text{m}$, $\gamma = 1000$, $N = 10^{10}$.

| $L$ m | $R$ m | $\gamma$ | $P$ W | $P^{(N)}_{\text{coh.}}$ W | $\gamma_{\text{crit.}}$ |
|---|---|---|---|---|---|
| 0.01 | 10 | 10 | 207 | 568 | 3336 |
| | | 100 | 555 | 571 | 3336 |
| | | 1000 | 563 | 571 | 3336 |
| | | 10000 | 563 | 571 | 3336 |
| 0.001 | 10 | 1000 | 12179 | 12298 | 7187 |
| 0.01 | 100 | 1000 | 121.8 | 123.0 | 7187 |

• confirmation

# UAL STRINGSC CODE



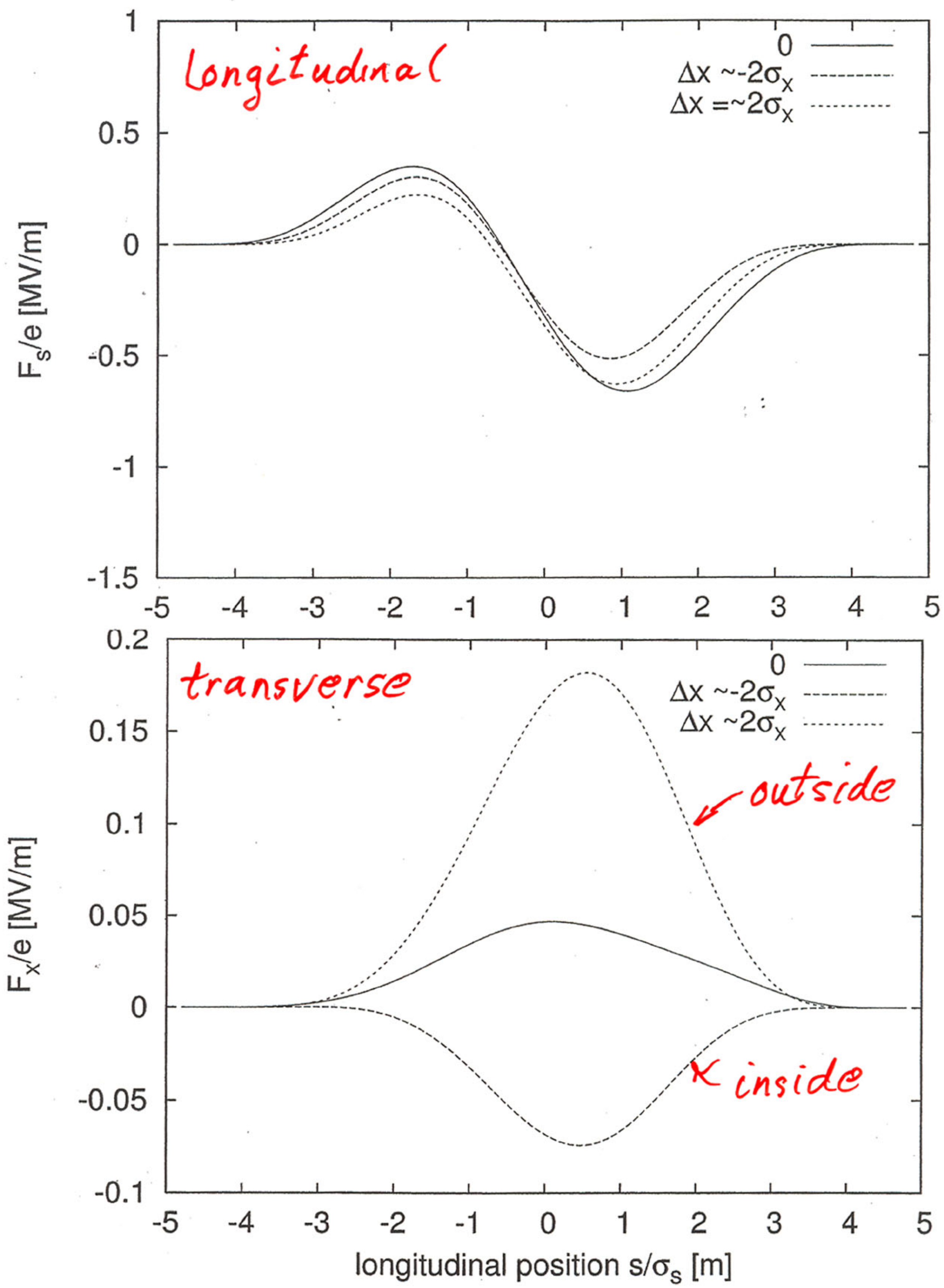


$Q = 1\,nC$, $\sigma = 50\,\mu m$, $\gamma = 100$

TRAFIC 4, Dohlus, Kabel, Limberg, NIM A, 445 (2000)

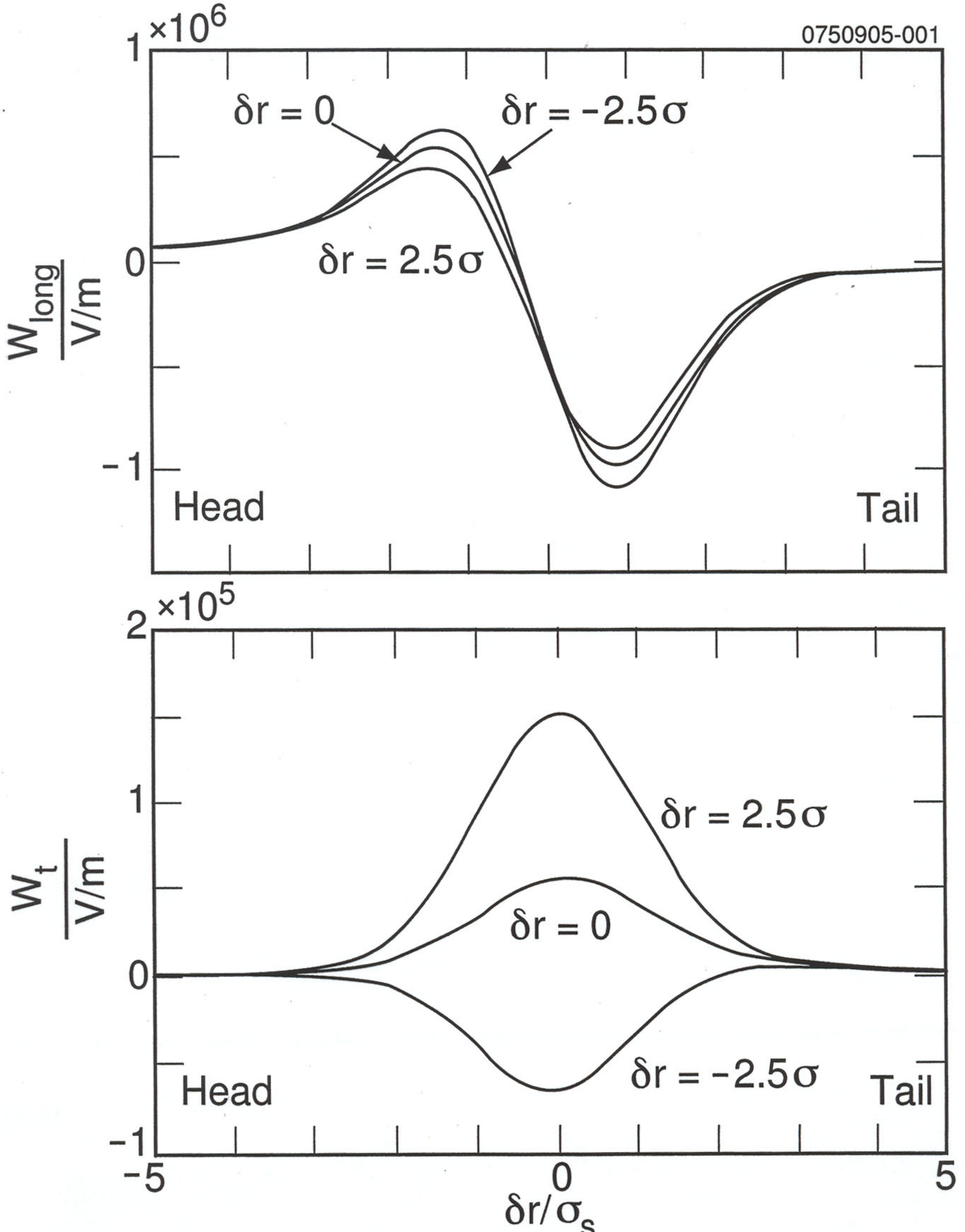


$Q = 1\,nC$, $\sigma = 50\,\mu m$, $\gamma = 100$

# CORNELL ERL CANDIDATE CONFIGURATIONS 

"SPROCKET"

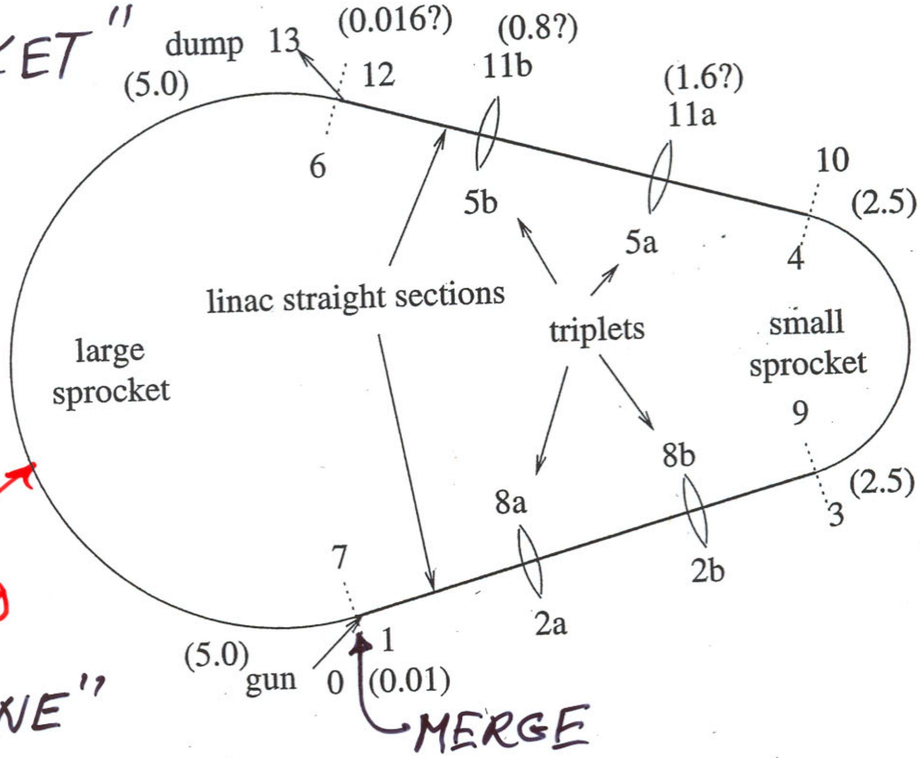


existing tunnel

"DOG-BONE"

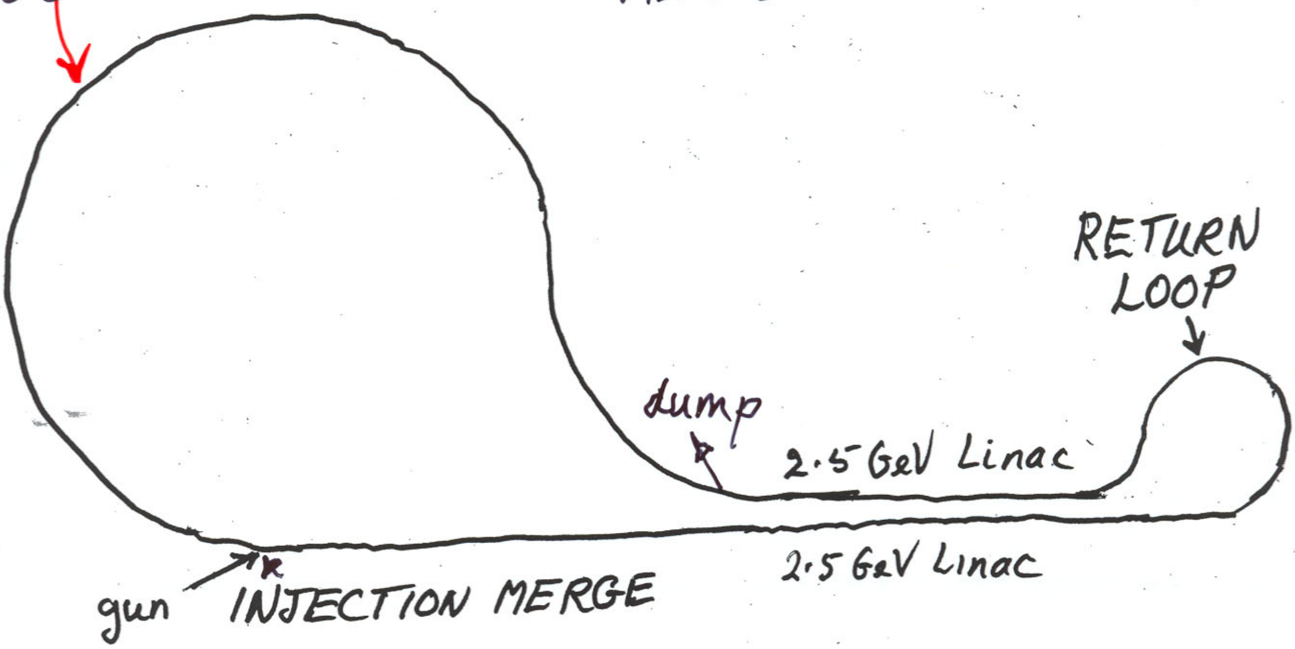

UAL stringsc simulation

qtot(C): 1e-09, Np: 300, Nturns: 1, seed: -100, ee(GeV): 2.5, ldh(m): 0.333, deltheth(r): 0.0164, lstr(mm): 0.2 LATTICE: return
xhW(micron): 50, yhW(micron): 50, cthW(mm): 0.5, dehW(%): 0.1: uniform longitudinal
IN : betax(m): 4.31, betay(m): 2.88, epsx(m): 5.78e-10, epsy(m): 8.35e-10
OUT: betax(m): 6.91, betay(m): 2.9, epsx(m): 1.02e-09, epsy(m): 8.35e-10

NOTE: VERTICAL AXIS LABELS ARE ON RIGHT

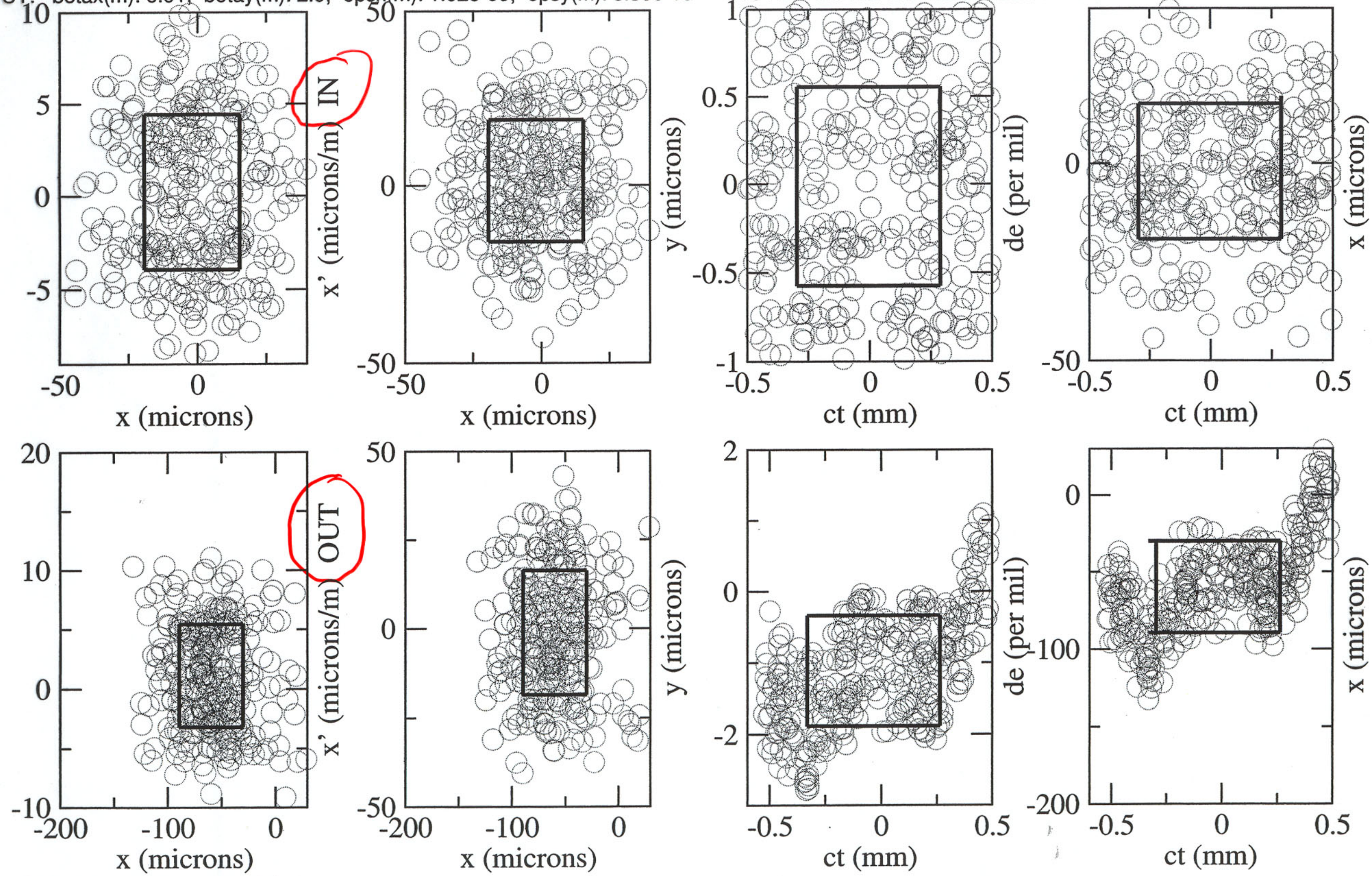


Sun Sep 25 19:51:30 2005

1nC, 2.5GeV, return loop

INVARIANT EMITTANCE AFTER 5 DEGREE INJECTION MERGE

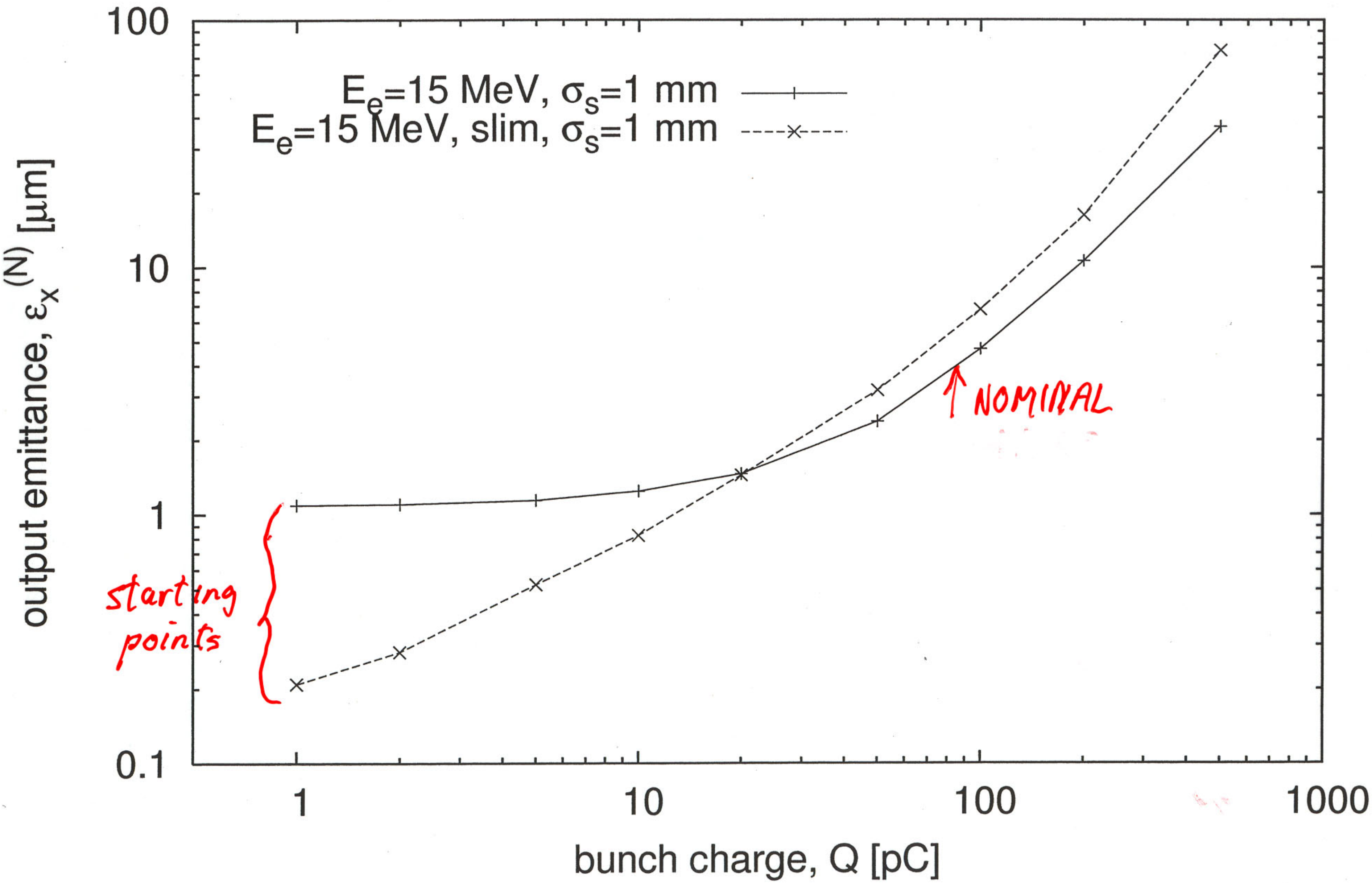

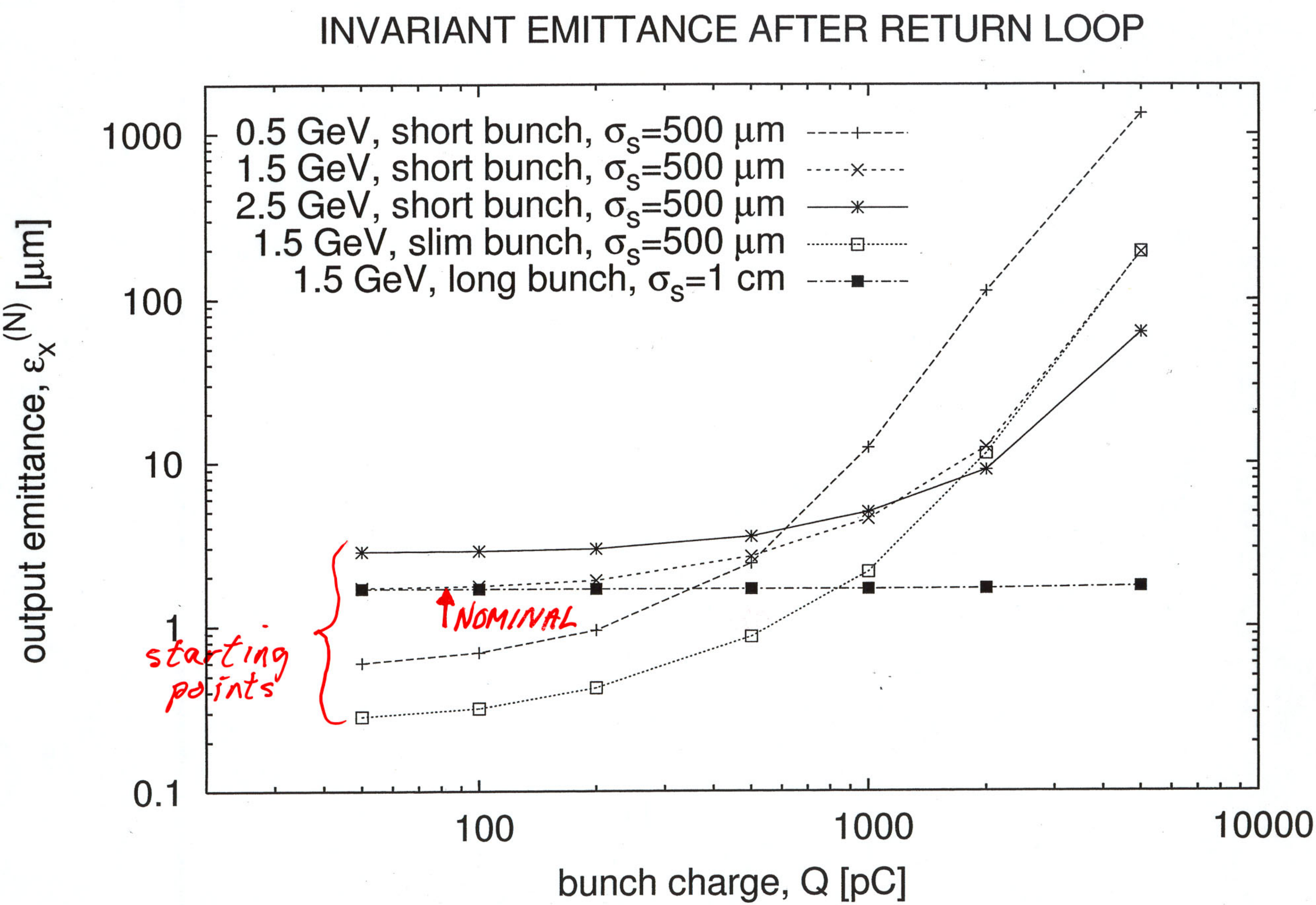

INVARIANT EMITTANCE AFTER RETURN LOOP
0.5 GeV, short bunch, $\sigma_s$=500 μm
1.5 GeV, short bunch, $\sigma_s$=500 μm
2.5 GeV, short bunch, $\sigma_s$=500 μm
1.5 GeV, slim bunch, $\sigma_s$=500 μm
1.5 GeV, long bunch, $\sigma_s$=1 cm
output emittance, $\varepsilon_x^{(N)}$ [μm]
bunch charge, Q [pC]
0.1
1
10
100
1000
100
1000
10000
NOMINAL
starting points


18

# Implication of CSR/CSCF for ERL Route

- Nominal values

  Charge/bunch 100 pC
  Emittance 2 μm

seem OK.

- Higher charge/bunch
  Lower emittance

$\left.\begin{array}{l}\text{Higher charge/bunch}\\ \text{Lower emittance}\end{array}\right\}$ probably not

#19

II (RAPID CYCLING) CESR UPGRADE TO HIGH BRIGHTNESS X-RAY SOURCE

ABSTRACT. "First generation" storage ring x-ray storage ring sources ran parasitically off radiation produced by electron accelerators designed for, and in use by, elementary particle physics. "Second generation" x-ray sources, for the first time, derived beams from "insertion devices" introduced into lattices for the specific purpose of producing external x-ray beams. The designs of "third generation" storage rings have been predicated entirely on their use as sources of x-rays. Mainly this means they have emittances far smaller than is useful for rings dedicated to elementary particle physics. Here we consider a "fourth generation" of sources made possible when a (large) tunnel and accelerator infrastructure is made available by the decommissioning of a colliding beam facility such as PEP, PETRA, CESR, and, eventually, even KEK. The constaints imposed by existing real estate constraints yield very different optimization considerations than are applicable to the design of an x-ray facilities built "from the ground up". Mainly this amounts to taking advantage of the "extavagantly" large circumferences of an inherited ring to produce major improvement of spectral brightness compared to existing third generation sources.

(PETRA3, ~~$~~275M, 6GeV
Construction begins: 2007
completion: 2009

ERL recovers 99%

present scheme duty factor = $10^{-6}$

# ALL THE ACCELERATOR PHYSICS YOU NEED TO KNOW

1. energy = voltage x current x time

2. Bending magnets (like plane mirrors) are optically inert

3. $\varepsilon$ = "emittance" = phase space area = spot_size x angular_divergence

4. Liouville's theorem: $\varepsilon^{(N)} = \gamma\,\varepsilon =$ "invariant emittance" where $\gamma = E/mc$^2
   = constant (except for synchrotron radiation)

5. $\varepsilon_x$ (equilibrium in storage ring) = constant $\times\ \gamma^2\theta^3$
   where $\theta$ = bend angle per magnet

6. $B$ = "spectral brightness" = photon density in 6D phase space = best figure of merit
   $$= \frac{2 \times 10^{18}\ I\,[\mathrm{A}]}{\varepsilon_x\,[\mathrm{nm}]\,\varepsilon_y\,[\mathrm{nm}]}\ \frac{N_w K^2}{1 + K^2/2}$$
   where $N_w$ = undulator number of periods
   $K$ = undulator constant $\overset{\text{e.g.}}{=}$ 1

7. Resonances and instabilities: accelerator physicists don't understand them either

F. 20

**The plan:**

- Build a new ultralow emittance storage ring in the Wilson tunnel (call it CESR' or CHESS') with storage time of ten seconds or so. The previous batch is kicked out at this rate and a new batch kicked in.
- These batches have been accelerated in a synchrotron SYNCH' largely reconstructed from the present CESR. (~ 2/3)
- The high performance Sinclair/Bazarov, ERL-intended gun and cryomodule currently funded ($16M) and under development are essential.

**Novel Feature:** Short storage time (to defeat Touschek effect.)

**Performance.**

- Spectral brightness (and hence) coherence from present day (few meter long) undulators:
  - $10^5 \times$ present CHESS
  - $10 \times$ present state of art for 3rd generation light sources
  - $10 \times$ proposed ERL (far more for hard x-rays)
  - $1 \times$ proposed ERL for round x-ray beams from 5 GeV electrons
- The number of these undulators possible is limited only by cost.

21

# THE PLAN (hypothetical)

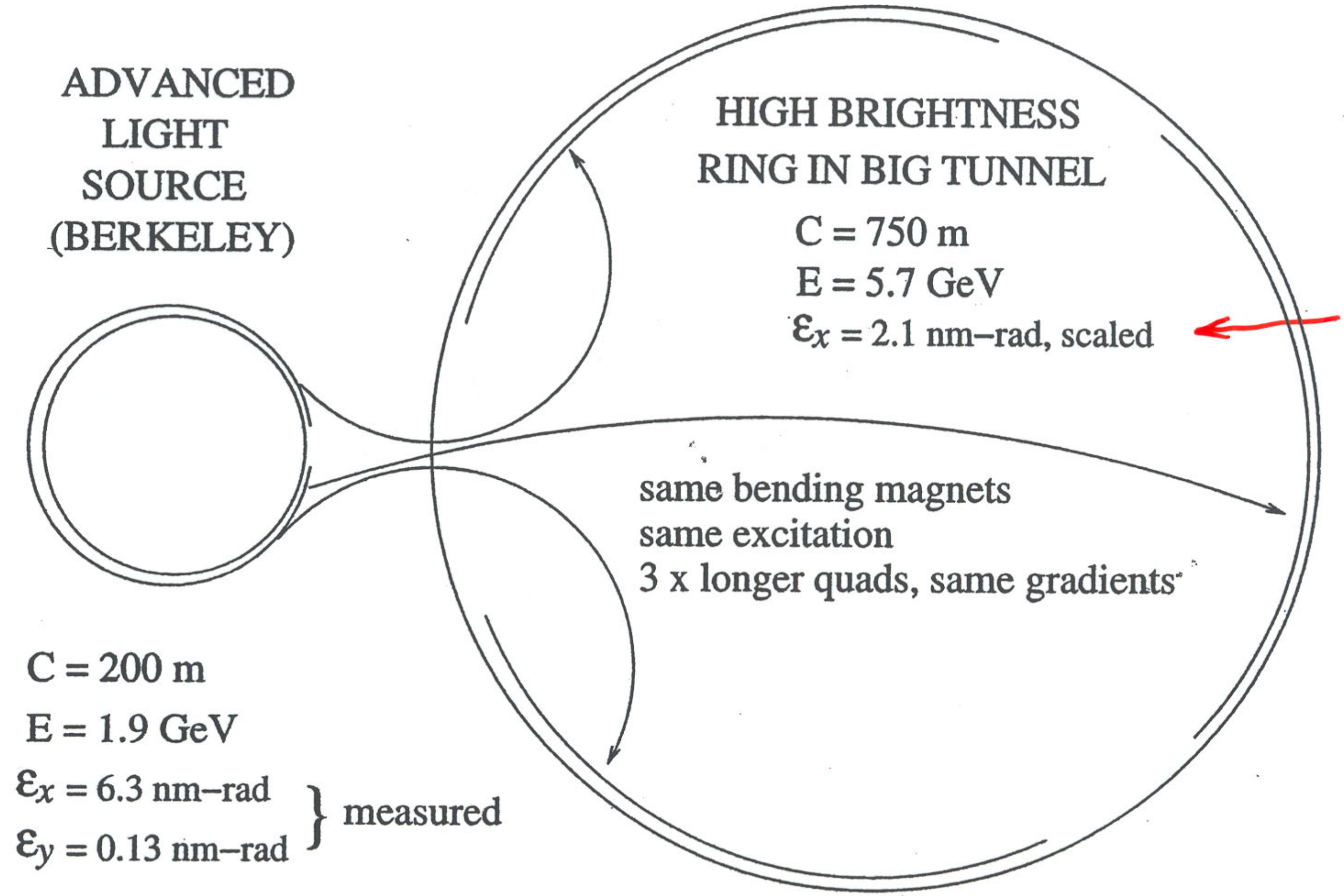


another factor of $\frac{1}{4}$ comes from minimum emittance design

FIGURE 4. Hypothetical triplication of the ALS 1.9 GeV storage ring to make a 5.7 GeV storage ring in a bigger tunnel.

Performance will be almost indistinguishable from ALS (3 times around)

# THE PLAN (actual)

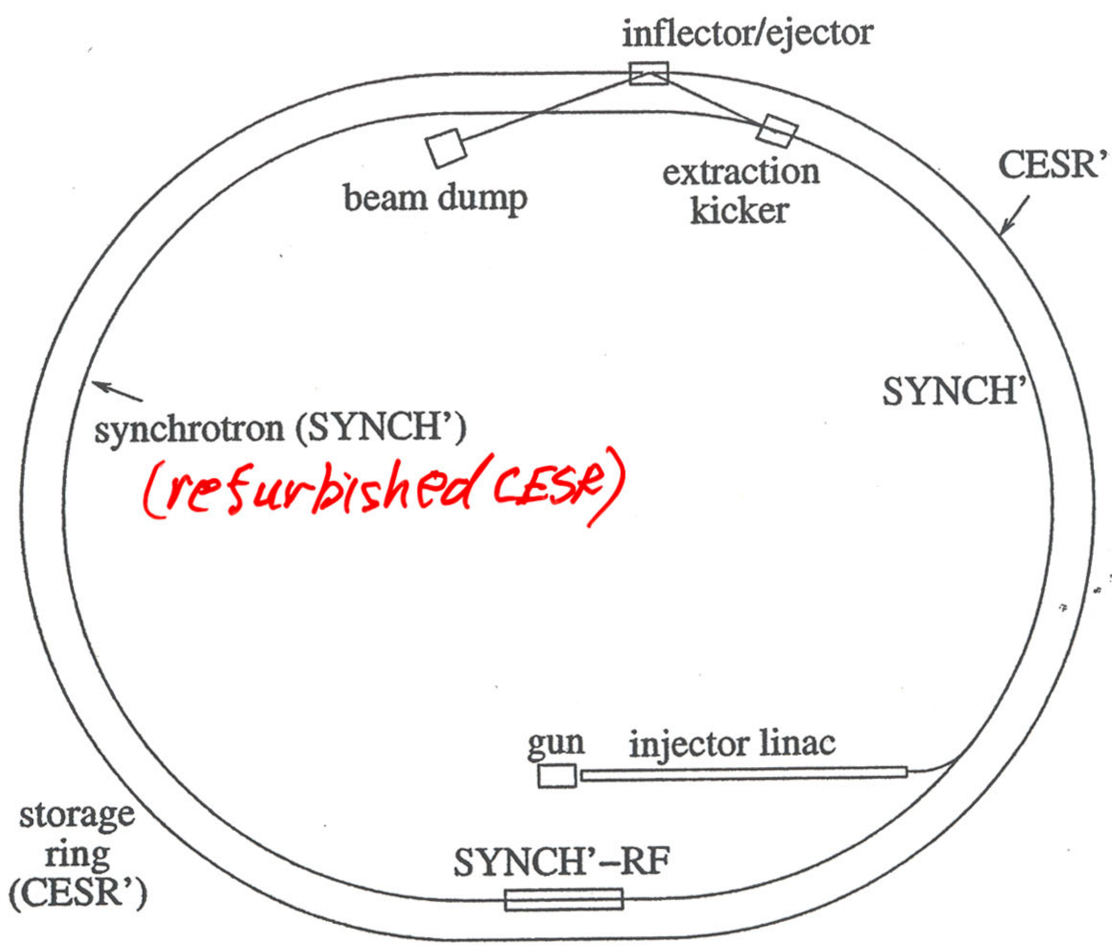


FIGURE 7. Schematic layout of the full acceleration system.

THE NOVEL FEATURE (fast cycling) beats ~~Touschek~~ intrabeam scattering

SYNCH'

CESR'

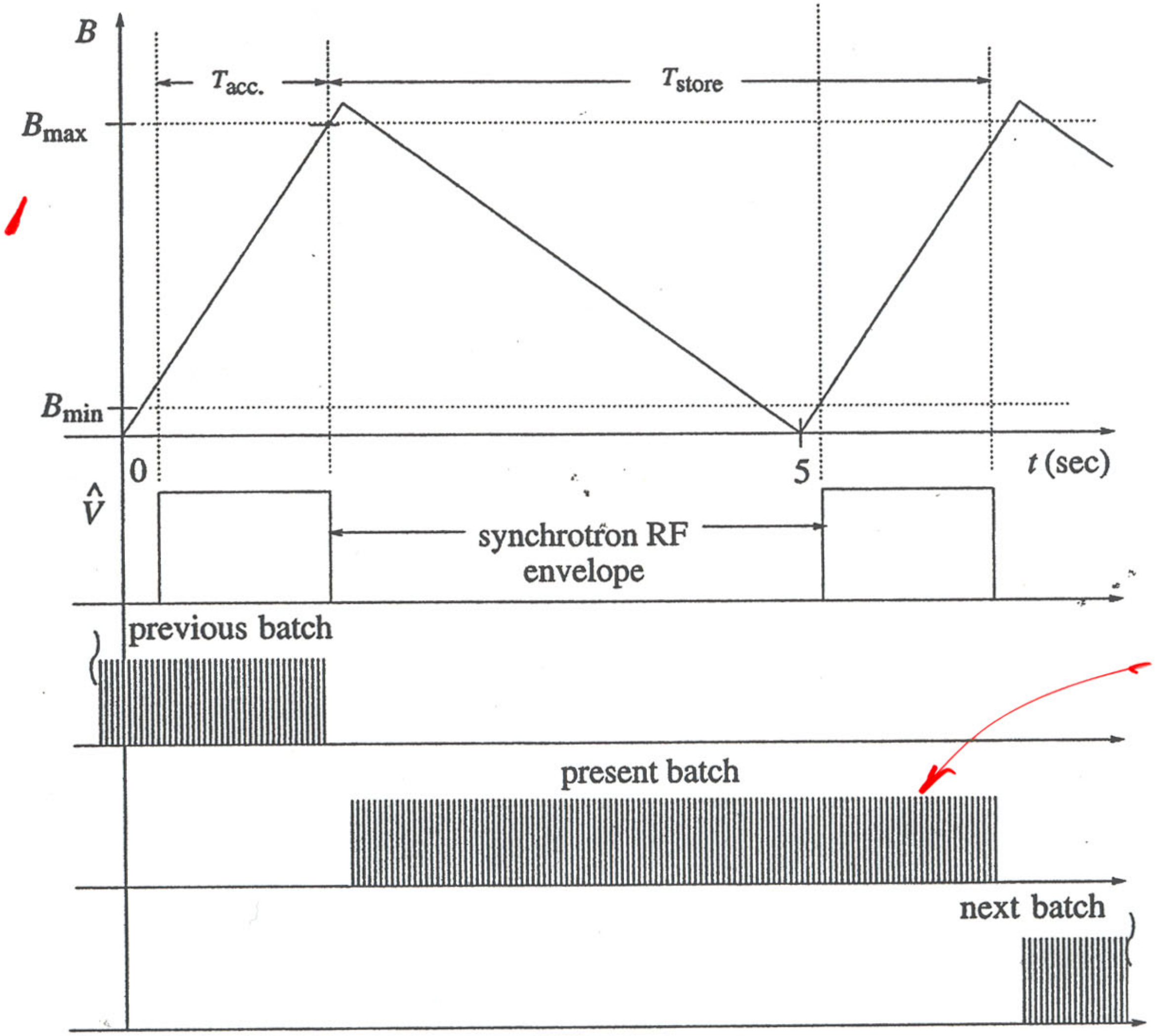


structure identical to Cornell-proposed ERL

FIGURE 8. Acceleration cycle showing the synchrotron (SYNCH') magnetic field, the SYNCH'-RF modulation $\hat{V}$, and the bunch pattern in CESR'/CHESS'. The cycle time $T_C$, labelled 5 s in the figure, is expected to be in the range from 2 to 20 seconds.

~~8.~~ 24

Φ: 25

FIGURE 6. Twiss and dispersion functions for one $L_C = 9\,\mathrm{m}$ cell of the proposed ultralow emittance storage ring CESR'. This forms one section of a multibend acromat (MBA).

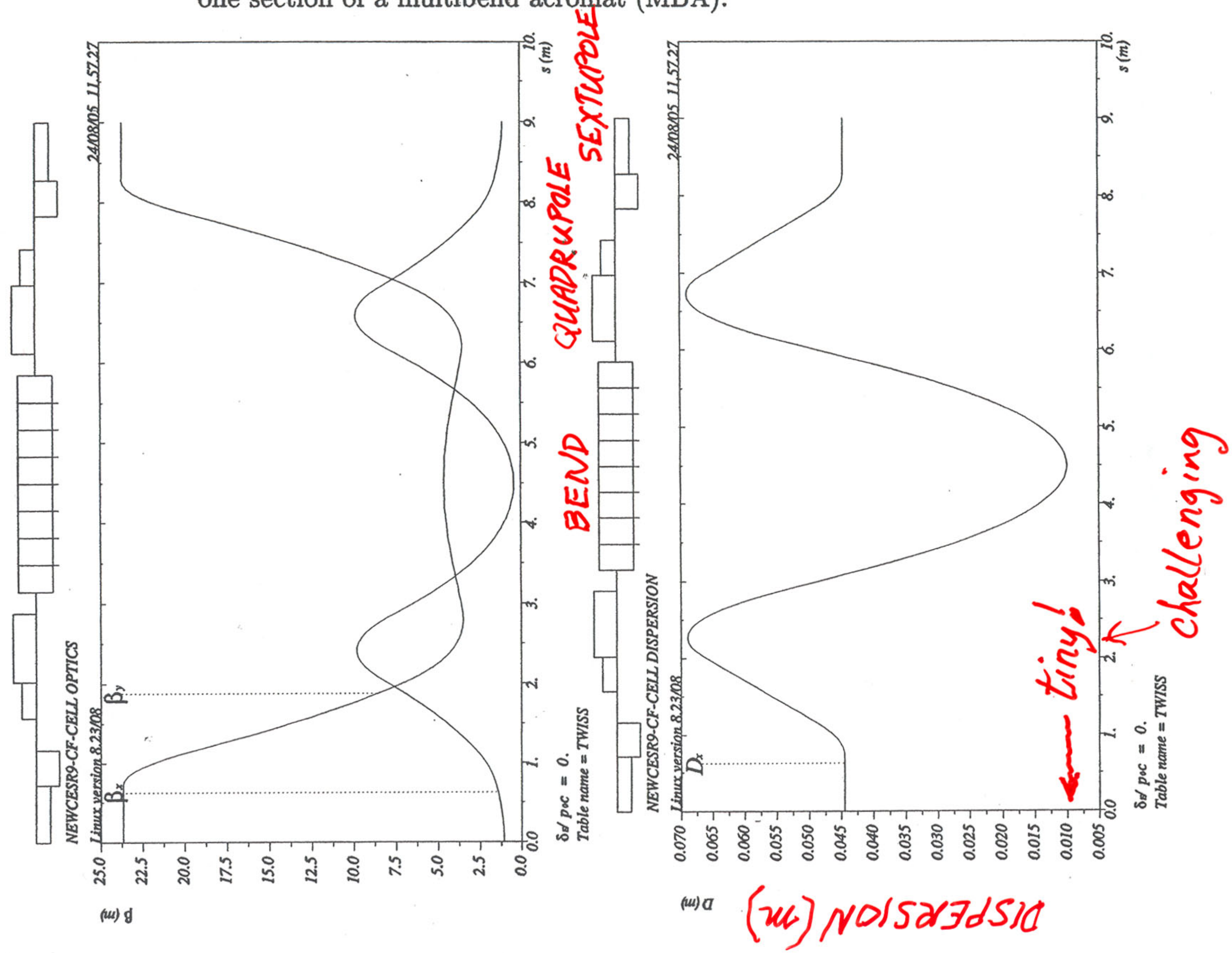

#26

FIGURE 5. Twiss and dispersion functions for the proposed ultralow emittance storage ring CESR'. The lattice functions for this complete lattice do not quite correspond to those in FIG 6 (dispersion suppression for that cell, which has combined function bends, has not been worked out). But the longitudinal spacing along the circumference more or less matches the tunnel geometry. To support more x-ray beamlines each sextant could be configured as two 5-bend achromats instead of as the 11-bend achromat shown.

Long undulator locations

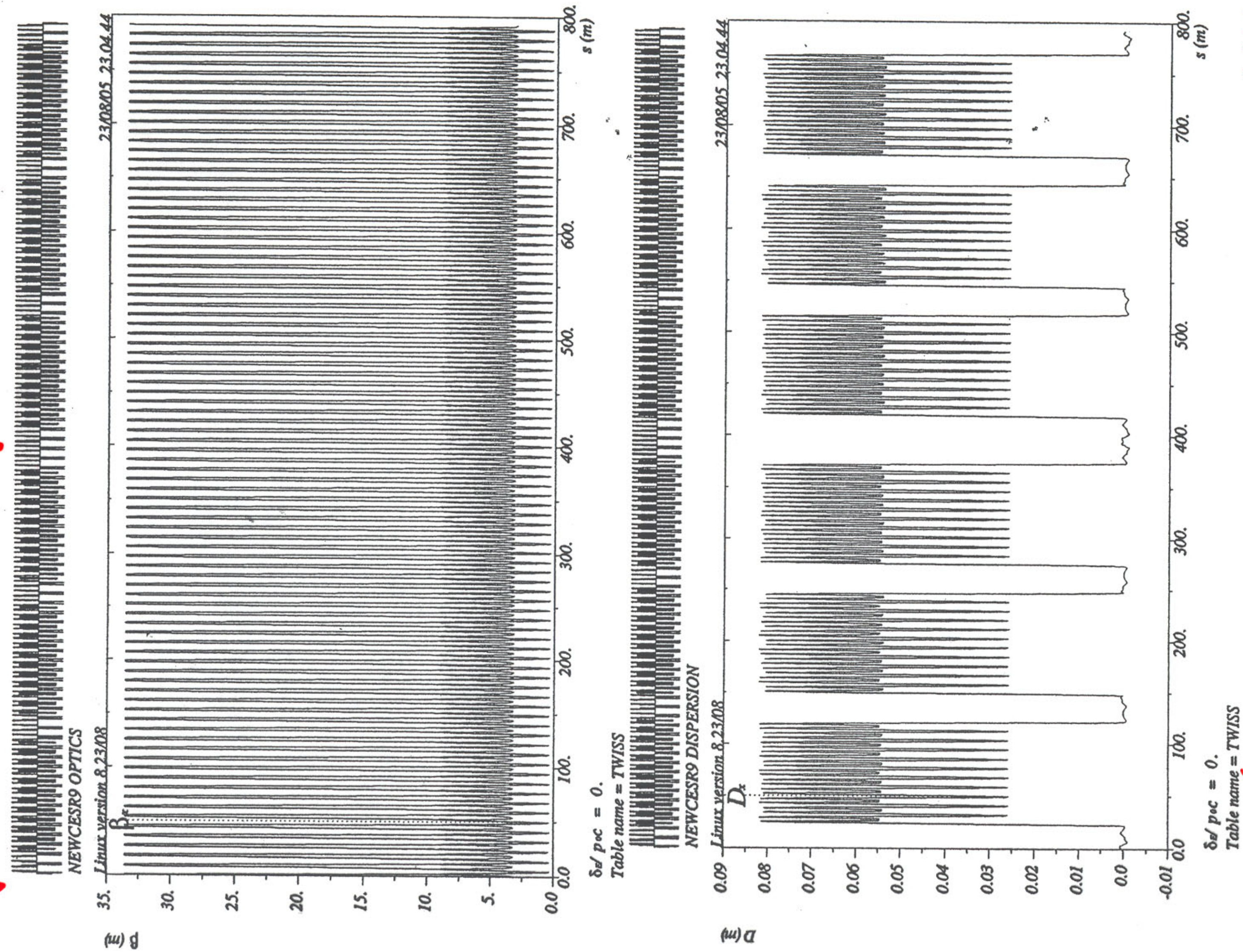


WILSON BLDG

TOWER ROAD

WILSON BUILDING

#27

TABLE 1. Numerical values for minimal emittance lattices of various cell lengths for $E_0 = 5\,\mathrm{GeV}$. The entries in `typewriter font` are in MAD units. Some 100 m (out of a $C = 750$ m tunnel circumference) have been reserved for straight sections and their contributions are not included in this table. In the rows labeled $J_x \epsilon_x$ one has $1.0 < J_x < 1.6$.

| parameter | unit | $L_C = 6$ m | $L_C = 9$ m | $L_C = 12$ m | $L_C = 15$ m | $L_C = 18$ m |
|---|---|---|---|---|---|---|
| | | | CESR' | | | SYNCH' |
| $N_C$ | | 110 | 72 | 54 | 42 | 36 |
| $C_a$ | m | 660 | 648 | 648 | 630 | 648 |
| $\theta$ | rad | 0.057120 | 0.087266 | 0.11636 | 0.14960 | 0.17453 |
| $\rho$ | m | 31.513 | 30.940 | 30.940 | 30.080 | 30.940 |
| $B$ | T | 0.52925 | 0.53906 | 0.53906 | 0.55446 | 0.53905 |
| $L$ | m | 1.8 | 2.7 | 3.6 | 4.5 | 5.4 |
| $l_{q1}$ | m | 0.300 | 0.450 | 0.600 | 0.750 | 0.900 |
| $l_{q2}$ | m | 0.570 | 0.855 | 1.140 | 1.425 | 1.710 |
| $l_{s1}$ | m | 0.480 | 0.720 | 0.960 | 1.20 | 1.440 |
| $l_{s2}$ | m | 0.300 | 0.450 | 0.600 | 0.750 | 0.900 |
| `ld2` | m | 0.180 | 0.270 | 0.360 | 0.450 | 0.540 |
| `ld1` | m | 0.270 | 0.405 | 0.540 | 0.675 | 0.810 |
| $l_2$ | m | 1.365 | 2.0475 | 2.730 | 3.4125 | 4.095 |
| $d$ | m | 1.005 | 1.5075 | 2.010 | 2.5125 | 3.015 |
| $l_1$ | m | 0.630 | 0.9450 | 1.260 | 1.575 | 1.890 |
| `k1[b], init.` | 1/m | -0.20 | -0.16 | -0.12 | -0.09 | -0.07 |
| $q_{1,thin}$ | 1/m | -0.66430 | -0.44287 | -0.33215 | -0.26572 | -0.22143 |
| $q_{1,thin}/l_{q1}$ | 1/m | -2.2143 | -0.98416 | -0.55358 | -0.35429 | -0.24603 |
| `k1[q1]`, thick | $m^{-2}$ | -2.4246 | -0.98578 | -0.55448 | -0.35480 | -0.24513 |
| $q_{2,thin}$ | 1/m | 1.33732 | 0.89155 not | 0.66866 | 0.53493 | 0.44577 |
| $q_{2,thin}/l_{q2}$ | 1/m | 2.3462 | 1.03232 so | 0.58654 | 0.37539 | 0.26068 |
| `k1[q2]`, thick | $m^{-2}$ | 2.7734 | 1.19642 bad | 0.67293 | 0.43048 | 0.29551 |
| tune, $\nu_x$ | | 87.12 | 53.93 | 38.77 | 29.61 | 24.52 |
| tune, $\nu_y$ | | 37.95 | 17.71 | 16.04 | 13.73 | 12.71 |
| $S_1$ | $m^{-2}$ | -35.27 | -9.384 | -3.800 | -1.900 | -1.120 |
| `k2[S1]`, thick | $m^{-3}$ | -147.0 | -26.07 | -7.917 | -3.167 | -1.555 |
| $S_2$ | $m^{-2}$ | 43.19 | 11.59 | 4.466 | 2.157 | 1.211 |
| `k2[S2]`, thick | $m^{-3}$ | 287.9 | 51.5 big | 14.89 | 5.752 | 2.691 |
| $\beta_0$ | m | 0.2324 | 0.3486 | 0.4648 | 0.5810 | 0.6971 |
| $\beta_{0,achieved}$ | m | 0.2302 | 0.4244 | 0.6645 | 0.8811 | 1.151 |
| $\eta_0$ | m | 0.00428 | 0.00982 | 0.01745 | 0.02805 | 0.03927 |
| $\eta_{0,achieved}$ | m | 0.00418 | 0.00995 | 0.02307 | 0.03363 | 0.05271 |
| $<\mathcal{H}>_{theory}$ | mm | 0.12636 | 0.44242 | 1.0487 | 2.1670 | 3.5393 |
| $J_x\,\epsilon_{x,theory,flat}$ | nm | 0.14742 | 0.52572 | 1.2461 | 2.6485 | 4.2057 |
| $J_x\,\epsilon^{(N)}_{x,theory,round}$ | $\mu$m | 0.77 | 2.57 | 6.1 | 13.0 | 20.6 |

"same" as ERL

#28

TABLE 2. Emittance evolution in synchrotron SYNCH', with its cell length taken to be $L_C = 18\,\mathrm{m}$, twice as great as in CESR'. The invariant emittance at injection is taken to be $\epsilon_x^{(N)} = 2\,\mu\mathrm{m}$. $\Delta E_e$ is the energy loss per turn and $\tau$ is a characteristic damping time. Transition from adiabatic damping dominance to radiation dominance occurs near the horizontal line part way down the table. Column 5 gives the aperture in units of the adiabatic damped beam size, which is applicable well above the line. The last column gives the aperture in units of equilibrium beam size, which is applicable well below the horizontal line.

number of σ's

almost ok

| $E_e$ GeV | $\Delta E_e$ MeV | $\tau$ s | $\epsilon_{in}$ m | $\sqrt{\epsilon_{accept}/\epsilon_{in}}$ | $\epsilon^{(N)}_{equi.}$ m | $\epsilon_{equi.}$ m | $\sqrt{\epsilon_{accept}/\epsilon_{equi.}}$ |
|---|---|---|---|---|---|---|---|
| 0.1 | 2.1E-7 | 1042 | 1.02E-8 | 8.65 | | | |
| 0.2 | 3.4E-6 | 130 | 5.11E-9 | 12.2 | | | |
| 0.3 | 1.7E-5 | 39 | 3.41E-9 | 15.0 | | | |
| 0.4 | 5.4E-5 | 16.2 | 2.56E-9 | 17.3 | 1.86E-8 | 2.37E-11 | 180 |
| 0.5 | 1.3E-4 | 8.3 | 2.04E-9 | 19.3 | 3.63E-8 | 3.71E-11 | 144 |
| 0.7 | 5.1E-4 | 3.0 | 1.46E-9 | 22.9 | 9.95E-8 | 7.26E-11 | 103 |
| 1.0 | 2.1E-3 | 1.04 | 1.02E-9 | 27.3 | 2.90E-7 | 1.48E-10 | 72 |
| 1.5 | 1.1E-2 | 0.31 | 6.81E-10 | 33.5 | 9.79E-7 | 3.34E-10 | 48 |
| 2.0 | 3.4E-2 | 0.130 | 5.11E-10 | 38.7 | 2.32E-6 | 5.93E-10 | 36 |
| 3.0 | 0.171 | 0.039 | 3.41E-10 | 47.4 | 7.83E-6 | 1.33E-9 | 23.9 |
| 4.0 | 0.541 | 0.0163 | 2.56E-10 | 54.7 | 1.86E-5 | 2.37E-9 | 18.0 |
| 5.0 | 1.32 | 0.0083 | 2.04E-10 | 61 | 3.63E-5 | 3.71E-9 | 14.4 |
| 6.0 | 2.74 | | | | 6.27E-5 | 5.34E-9 | 12.0 |
| 7.0 | 5.07 | | | | 9.95E-5 | 7.26E-9 | 10.3 |
| 8.0 | 8.65 | | | | 1.49E-5 | 9.49E-9 | 9.0 |

almost ok

TABLE 3. Emittance evolution and aperture requirements in CESR'. The emittance $\epsilon_{in}$ column four of this table is copied from the $\epsilon_{equi.}$ entry in the second last column of Table 2.

| $E_e$ GeV | $\Delta E_e$ MeV | $\tau$ s | $\epsilon_{in}$ m | $\sqrt{\epsilon_{accept}/\epsilon_{in}}$ | $\epsilon^{(N)}_{equi.}$ m | $\epsilon_{equi.}$ m | $\sqrt{\epsilon_{accept}/\epsilon_{equi.}}$ |
|---|---|---|---|---|---|---|---|
| 1.0 | 2.1E-3 | 1.04 | 1.48E-10 | 50.8 | 3.62E-8 | 1.85E-11 | 144 |
| 1.5 | 1.1E-2 | 0.31 | 3.34E-10 | 33.8 | 1.22E-7 | 4.17E-11 | 96 |
| 2.0 | 3.4E-2 | 0.13 | 5.93E-10 | 25.4 | 2.90E-7 | 7.41E-11 | 72 |
| 3.0 | 0.171 | 0.039 | 1.33E-9 | 17.0 | 9.79E-7 | 1.67E-10 | 47.9 |
| 4.0 | 0.541 | 0.0163 | 2.37E-9 | 12.7 | 2.32E-6 | 2.97E-10 | 35.9 |
| 5.0 | 1.32 | 0.0083 | 3.71E-9 | 10.1 | 4.53E-6 | 4.63E-10 | 28.7 |
| 6.0 | 2.73 | 0.0048 | 5.34E-9 | 8.46 | 7.83E-6 | 6.67E-10 | 23.9 |
| 7.0 | 5.07 | 3.0E-3 | 7.26E-9 | 7.26 | 1.24E-5 | 9.08E-10 | 20.5 |
| 8.0 | 8.65 | 2.0E-3 | 9.49E-9 | 6.34 | 1.86E-5 | 1.19E-9 | 18.0 |

not quite ok

TABLE 4. Comparison of spectral brightnesses $\mathcal{B}$ for various storage-ring-plus-undulator x-ray sources. "RC" stands for the present rapid cycling proposal. For this and for the Cornell-ERL case, a 4 meter long, 117 pole, $K = 1$, undulator, with $\lambda_w = 3.4$ cm, is assumed, and Eq. (6) is used to calculate $\mathcal{B}$. All entries are in (standard) units for spectral brightness, as given in that equation. The ESRF and SPRING-8 undulators are similar, but different, and the entries are published values for $\mathcal{B}$. Cases with $\sim$ symbols are obtained by crude scaling. Some possible sources of overestimate in the RC, 5 GeV-flat column are discussed in the next section. For these, and all other estimates, the horizontal partition number has been taken to be $J_x = 1$. It may be possible to increase the RC brightnesses by as much as a factor of two by tuning to $J_x \approx 1.5$, as is done at ALS and CLS.

| $E_\gamma$ keV | n | RC 5 GeV 4 m | RC 8.1 GeV 4 m | RC 5 GeV 4 m | Cornell-ERL 5 GeV 4 m | ESRF, U35 6 GeV | SPRING-8 8 GeV 5 m |
|---|---|---|---|---|---|---|---|
| | | flat | flat | round | round | flat | flat |
| 4.7 | 1 | 7.3E21 | | 2.9E20 | 3.7E20 | 6E20 | |
| 14 | 3 | ~6E21 | | ~3E20 | ~3E20 | 5E20 | |
| 23 | 5 | ~5E21 | | | | | |
| 12.4 | 1 | | 1.1E22 | | | | 6E20 |
| 37.2 | 3 | | ~1E22 | | | | 5E20 |

#29

# Conclusions Concerning Rapid Cycling Conventional Technology Route

Pro's

- brightness
  - round beam – same as ERL
  - flat beam – 10 × ERL
- cost far less than ERL
- power far less than ERL
- little new civil construction

Con's

- femtosecond bunches impossible
- very long undulators impossible